DOI: 10.1002/masy.200651319

X-Ray Study of *Herbaspirilum Seropedicae* GlnB Protein Adsorbed on Silicon

Adriana Freire Lubambo,[1] *Elaine Machado Benelli,*[2] *Irineu Mazzaro,*[1]
Fabiano Yokaichyia,[3] *Carlos Giles,*[4] *Paulo César de Camargo**[1]

Summary: GlnB-Hs protein is a globular member of PII-like family involved in the nitrogen control fixation in diazothoph organisms like *H. seropedicae*. In this work, GlnB-Hs is deposited by spin-coating on Si (111) and its self-assembling is investigated by AFM (atomic force microscopy) and X-ray at grazing incidence angles. GlnB-Hs forms circular 100 nm to 150 nm wide face-up donut shaped protein aggregates on silicon. Reflectivity and diffraction profiles from the protein deposits on Si(111) and Si(100), suggest ordered domains that are stable under the X-ray beam and have d-spacing compatible with protein dimensions already determined by classical protein crystallography.

Keywords: adsorption; atomic force microscopy (AFM); biopolymer; globular protein GlnB-Hs; self-assembly; X-ray

Introduction

In the last few years, the study of protein adsorption at various interfaces has shown an increasing interest. The driven forces that rule protein adsorption have been investigated by numerous techniques because of the important and wide number of applications that range from biocompatibility, biosensor design, to ultra filtration membranes.[1,2] One appealing interest is the use of nanobiofilm templates for protein crystallization and protein structure determination.[3,4]

The knowledge of protein structure has biochemical and biotechnological motivations: Structure is related to protein function, which means the ability of the protein to perform one special task, and the knowledge of protein function, leading us directly to the understanding of biological processes. So far, protein crystallization is a difficult and laborious task: it depends on finding the ideal conditions of the solution, which will allow crystallization and the results, are often unpredictable and irreproducible, resulting on crystals that have quality and dimensions often inappropriate to structural X-ray studies. When the crystal is formed, it is fragile due to weak interactions between proteins in the crystal lattice and has to be embedded in solvent solution to avoid cracking.[5] Furthermore, there are proteins reluctant to crystallize, for example, the knowing difficulty to prepare 3D crystal of membrane protein.[6]

X-ray surface methods on the study of organic monolayers and lipid monolayers on liquid and solid interfaces have demonstrated its capability to extract information of structure and ordering.[7–11] Also, this technique was successfully applied for structure determination of a single protein layer on liquid interface.[12] The investigation of protein thin film adsorbed on solid surface demands the use of strong radiation sources due to the small amount of material on the substrate (protein coverage of a few monolayers). The use of grazing incidence

---

[1] Department of Physics, Universidade Federal do Paraná, Curitiba, Brazil
E-mail: camargo@fisica.ufpr.br
[2] Department of Biochemistry and Molecular Biology-Universidade Federal do Paraná - Curitiba, Brazil
[3] Instituto de Física, Unicamp, Campinas, Brazil
[4] BNLS-Synchroton light source, Upton, USA

X-ray techniques is a promising tool, because it has the advantage of allowing the investigation of single layer crystalline order, with high resolution and sensitivity. This sensitivity is due to special X-ray beam conditions: the reason is that at grazing incidence angles, the beam is under total reflection and the evanescent wave only penetrates 100 Å or less, allowing the investigation of the thin film weak diffraction pattern without the contribution of the substrate.

Among several deposit techniques available to achieve a homogeneous and ordered protein layer on solid surface, the spin coating technique has being successfully used.[11] Due to the physical forces involved in the process, the formation of uniform layers is a natural consequence.[13]

The GlnB protein is a globular member of PII-like protein family, being present in Archaea, Bacteria and Eukarya, and it is a signal transduction protein involved in the control of nitrogen fixation in *H. seropedicae*, a diazotroph organism. This organism can be isolated in rice, corn, sorgo roots and also in sugar cane, banana and pineapple stems.[14–20]

The purpose of this study is the investigation of GlnB-Hs protein thin film ordering on silicon surface, using the spin coating technique with three kinds of deposit protocols. X-ray diffraction at grazing incidence angles is applied to detect any diffraction patterns and the results are compared to the crystallographic data already obtained for this protein. Atomic force microscopy (AFM) is also used in order to determine protein aggregates topography, that is, any conformational protein arrangement information after deposition on the substrate.

Material and Methods

Protein Preparation

This GlnB-Hs was purified as described by Benelli[21] and the structure was determined by X-ray diffraction.[22] The GlnB-Hs has a trimer structure (36 kDa) with one central and three lateral cavities with hydrophilic boundaries. The protein main dimensions are roughly 5 nm wide and 3 nm high.

Substrate and Surface Preparation

Standard commercial silicon wafers of p-type, boron doped, Si(111) and Si(100) orientation, 450 micrometers thick, were used as solid supports. The substrates were cleaved into 1-cm^2 pieces with a diamond-tipped scriber. After cleavage, the substrates were cleaned, before the protein deposition, in a boiling solution[23] of H_2O: H_2O_2: HCl (86:11:3) for 10 minutes, and dipped into H_2O: H_2O_2: NH_4OH (4:1:1) for another 10 minutes, preserving the SiO_2 oxide layer and maintaining the hydrophilicity of the silicon surface. Ultrapure water (Millipore, MilliQ, 18.2 $M\Omega \cdot cm$) was used in the cleaning solution and for rinsing abundantly the silicon surface after the cleaning process.

Protein Adsorption Protocols

The protein solution was diluted in a buffer solution of 50 mM Tris/HCl pH 8, 50 mM NaCl, 0.1 mM EDTA and 10% glycerol.[19] The silicon (100) and (111) surfaces were incubated with 10 μl drop of this freshly prepared 10 nMol buffered protein solution, keeping this adsorption protocol at room temperature. The excess of protein was eliminated by washing three times with 20 μl of 10 mM Tris/HCl pH 8 solution. The samples were then left to dry in air under controlled temperature (23 °C) and humidity conditions (45%), before X-ray analysis.

Three kinds of deposits (Table 1) on the plate were performed for each silicon surface orientation: In the first case, a drop of 10 μl buffered protein solution was centrally pipetted onto the rotating substrate at 2500 rpm, and then the substrate was washed with buffered solution three times. In the second case, the same drop size was deposit centrally at 1000 rpm, allowed to adsorb during 30 seconds; after deposition, the substrate was accelerated to 2500 rpm and then the washing process with buffer solution was repeated all the same.

Table 1.
List of investigated protein deposits.

Sample	Protein amount (μg/μL)	Buffer amount 3X (μL)	Step 1 Protein deposition Substrate speed (rpm)	Step 2 Adsorption time(s)	Step 3 Washing substrate speed (rpm)	Reapeating protocol
Si(111)F	35,97	20	2500	no	2500	no
Si(111) B	35,97	20	1000	30	2500	no
Si(111) L	35,97	20	1000	30	2500	yes
Si(100) 1	35,97	20	2500	no	2500	no
Si(100) 2	35,97	20	1000	30	2500	no
Si(100) 3	35,97	20	1000	30	2500	yes

The third kind of deposit was the same as the second one, except that after the washing step, the plate was de-accelerated to 1000 rpm again and a second drop of protein solution was deposited and allowed to adsorb another 30 seconds. After deposition, the excess of protein was eliminated as described above for the two preceding deposits.

Atomic Force Microscope Analysis

AFM imaging was performed at room temperature (~24 °C) using a commercial Shimadzu SPM-9500J3 microscope. Images were taken in the dynamic tapping mode (TM-AFM) with an oxide-sharpened micro fabricated silicon Olympus cantilever with a nominal spring constant of 30 N/m and a 10 nm tip radius of curvature. The scanning rate was 1 Hz and 256 × 256 data points were acquired. Image data were flattened after acquisition and some filter treatment was used when necessary. The operating point was adjusted to minimize the interaction and to avoid protein soft layer deformation.

X-ray Diffraction Analysis

Sample Data Collecting Parameters

The experiment was conducted on a Huber Six-Circle diffractometer, at XRD2 beamline (LNLS-Brazil), with monochromatic energy tuned to 7 keV, energy bandwidth ($\Delta\lambda/\lambda = 2.62 \times 10^{-4}$) and a focused beam. The vertical and horizontal slits were adjusted to have a footprint area of incomming X-ray beam illuminating all the silicon length (1cm) and having a width of 1mm and vertical divergence was 1.6×10^{-4} rad. The effects of beam radiation were avoided keeping the X-ray shutter open only during data collection. Scans were repeated in order to verify beam effects and ensure data reproducibility. The initial scattering profiles of standard θ-2θ in grazing incidence geometry were obtained using a scintilation counter (cyberstar) and image plate. All the measurements were made at room temperature. Scattering profiles were also obtained without protein deposit to be used as reference.

Data Treatment

All diffraction profiles have been corrected for storage ring current. The scattering profile of the reference silicon was used for control and the program IMD 4.1.1 was used to fit the experimental data.[24] All the reflectivity profiles fits were obtained using a two-layer model (silicon oxide layer, protein layer). Experimental data was fitted using the model parameters listed on Table 2. Error function was used to model the interface profile function.

Table 2.
Model parameters and fitting results.

Sample	Layer	Thickness t (Å)	Roughness σ (Å)
Si(111) F	Protein layer	30	5.0
	oxide layer	12.5	5.6
	Silicon		2.3
Si(111) B	Protein layer	30	5.0
	Oxide layer	12.5	5.6
	Silicon		2.3
Si(100) 2	Protein layer	50	5.6
	Oxide layer	22	5.6
	Silicon		1.0
Si(100) 3	Protein layer	50	5.6
	Oxide layer	22	5.6
	Silicon		1.0

Results and Discussion

GlnB-Hs forms circular donut shaped protein aggregates with dimensions varying from 100 nm to 150 nm widths and up to 3 nm high (Figures 1a and 1b), when deposited on silicon. These large circular protein aggregates are also formed by donut shaped arrangements of protein units with average width of 10 nm. Considering tip deconvolution, it is found that these units have 5 nm width and 3 nm height, in agreement with the protein structure already determined. Their arrangement on silicon (111) is essentially face-up donut shape configuration.[25]

θ-2θ scans were performed in order to observe possible diffraction pattern by single-crystals domains formed by these circular aggregates. The structural information along the direction perpendicular to substrate arrangement of these monolayers was obtained with the geometry such that, the incident and reflected angles are the same $\alpha_i = \alpha_r = \alpha$ and ($2\theta_{xy} = 0$). The scattering vector is $|q_z| = 2|k|$ senα.

The Si (111) reflectivity profiles (Figure 2a) have a large oscillation region $0.2\ \text{Å}^{-1} < \mathbf{q_z} < 0.6\ \text{Å}^{-1}$. This large oscillation is related to the fact that there are only a few monolayers and they are not uniform over the illuminating area.[11,25]

The protein layer thickness for samples Si(111)F and sample Si(111)B according to the fitting above is estimated to be 30 Å.

The Si (100) reflectivity profiles also showed a similar behavior (Figure 2b). The large oscillation is located at $0.2\text{Å}^{-1} < \mathbf{q_z} < 0.7\text{Å}^{-1}$ and the protein layer thickness for samples Si(100)2 and sample Si(100)3 is estimated as 50 Å.

For the sample Si(111) L, Figure 3a, a diffraction peak appeared at 0.194 Å^{-1}. Bragg's law gives a d-spacing of 32 Å, which is compatible with protein crystallographic data already determined for this protein.[22] Accordingly to Scherrer approach,[26] the broadening of diffraction peaks is due to the finite size of ordered domains. For this samples the FWHM is 0.97Å^{-1} giving an ordering domain around 60 Å corresponding to a stack of 2 proteins. Sample Si (100) 1 also showed a diffraction peak located at 0.157 Å^{-1}, giving ad- spacing of 39.97 Å with a FWHM corresponding to a stack of 6 proteins.

These 2D ordering domains formed could explain and be related to the mechanism of fast crystal growth using nanotemplate crystallization.[27,28] In our case, the 2D protein GlnB-Hs ordering arrays were formed by using the spin-coating technique.[11] The physical mechanism involved in 2D ordered arrays are

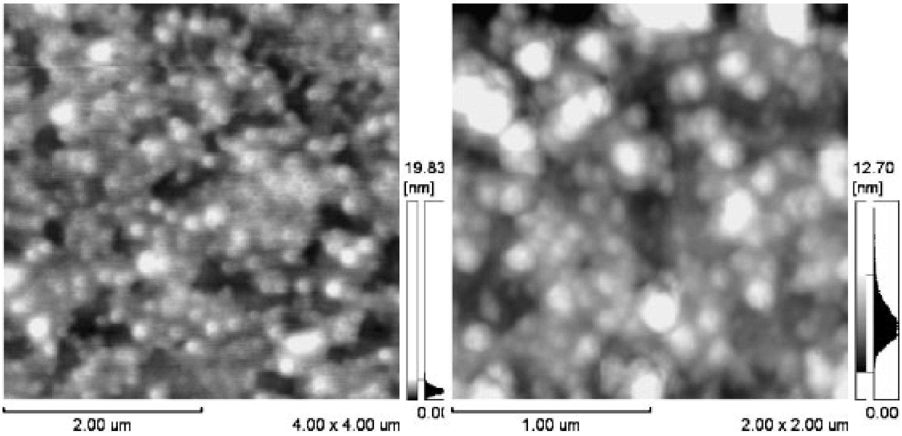

Figure 1.

(a). AFM images on dynamic mode of protein GlnB-Hs aggregates on Si(111), 10 nmol, 1000 rpm. (b). Zoom of image (a). Aggregates are essentially face-up donut shape configuration.

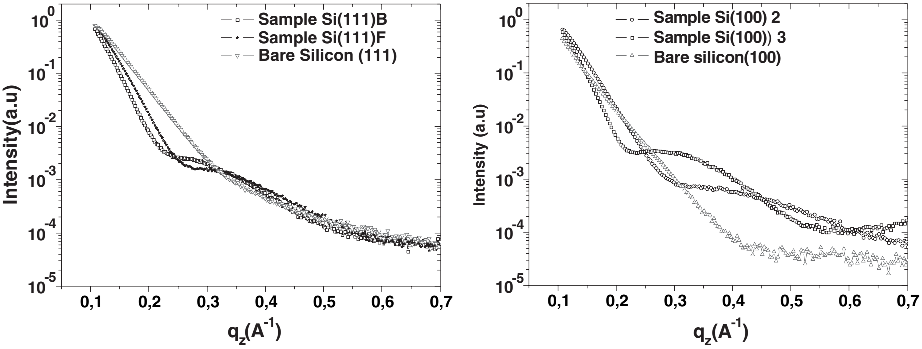

Figure 2.
Reflectivity profiles: (a) Silicon (111) and (b) Silicon (100) as a function of deposit conditions and reflectivity profile of bare silicon (on red) for control, scans at room temperature.

closely related to the attractive capillary immersion forces and convective particle flux acting during evaporation of wet thin films of colloid particles.[28,29]

Radiation damage to the sample was monitored performing two scans in the same region in order to detect any changes. The sample alignments were optimized to spend few minutes aligning and about 10 minutes scanning, resulting on no outstanding changes in diffraction profiles, within an interval of 20 minutes. For sample Si(100)1, azimuthal) (φ) scans with 10 degrees steps till 360° were performed to analyze the peak located at $q = 0.31$ Å^{-1}.

It was noticed that this peak was very stable under the beam. As shown (Figure 3), there was only 1.6% change in peak position to a greater d-spacing (unit-cell volume increasing is one of the characteristic effects of radiation damage[30]) and 20% decay in integrated intensity after 5 hours of total data collection at room temperature.

Small crystal domains may be more stable than large ones, because damage is proportional to the absorbed energy, rather than to amount photons absorbed, when the following conditions are fulfilled: there is no vicinity to an absorption band, energy due to Compton scattering is negligible, X-ray beam transmission is high and crystal is small enough to allow photoelectrons to leave the sample, carrying out a significant amount of energy.[31] In fact, as a first approach, when the path length of a

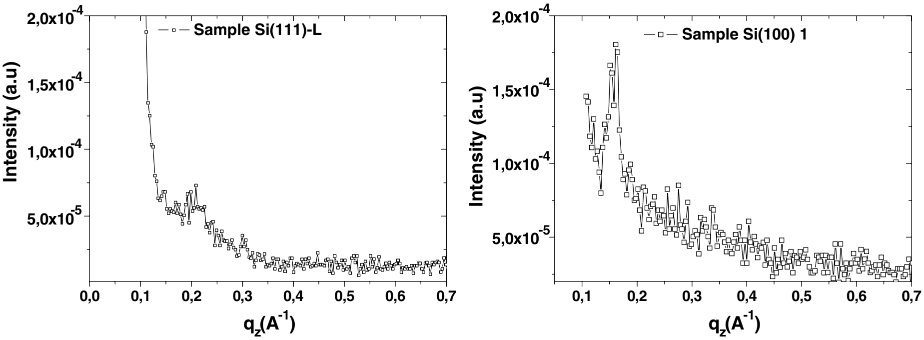

Figure 3.
(a) Sample Si (111)L and (b) Sample Si (100)1 showing a diffraction peak related to protein GlnB-Hs dimensions at 0.194 Å^{-1},d = 32 Å for Si (100) and at 0.157 Å^{-1},d = 39.97 Å for Si(100).

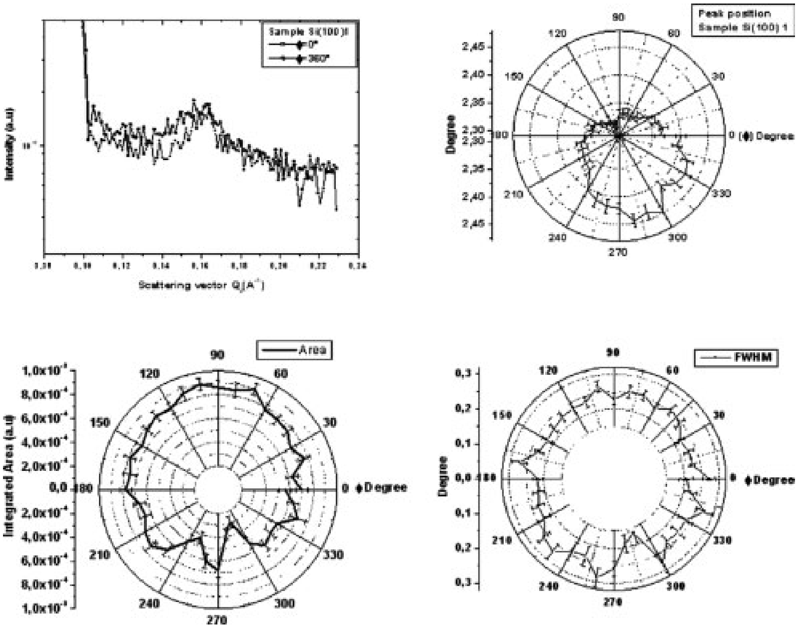

Figure 4.

(a). Sample Si(100) 1 diffraction peak at q = 0.31Å^{-1}, initial scan at azimuthal angle ($\phi = 0°$) and final scan at ($\phi = 360°$). (b). All angular (2θ) peak positions for the scans performed at ϕ positions. (c). Integrated area for all azimuthal scans. (d). Corresponding FWHM for all azimuthal scans performed on (c).

photoelectron is greater than protein crystal size, the absorbed radiation dose is reduced due to absence of Compton scattering, which contributes to incoherently energy emission.[23] In the case of this diffraction peak, as mentioned above, crystal domains of 246 Å are found in this sample. Using the Ashley approach which predicts values for electron mean free paths for 100 eV $\leq$ E $\leq$ 10 keV within 10% for organic insulators we find $\lambda \approx 500$ Å.[32]

This result means that for this energy (7 keV) and with this ordered domain size, the photoelectrons interaction is negligible. In addition, the distance traveled by the electron after a certain loss of energy (the collision stopping power) predicts roughly a electron loss of energy of 2.917 eV $\cdot$ Å^{-1}, giving a total energy deposit of 717.58 (eV) inside of a 246 Å ordered domain.[33] Monte Carlo simulation program Casino, shows that for the case of a small crystal of 250 Å, the electron created inside the crystal emerges out carrying out almost all energy.[34] Furthermore, if we think that the probability to have ordered domains without defect is greater when we have small domains, it means that more crystal domains are perfect resulting on dominant elastic scattering. As a direct consequence, we will have less energy dissipated into the crystal contributing to ionization, thermal heating, etc.[35] It is also important to remark that heavy element has a significant absorption cross-section, and it is known that primary radiation affects preferentially heavy absorbing atoms.[30] GlnB-Hs protein has only two sulfur atoms per monomer and no disulfide bonds, therefore, having small absorption cross-section. All these facts probably contribute to protein crystal domain stability under the X-ray beam.

Conclusion

GlnB-Hs protein crystal domains ordered along perpendicular direction are likely to be formed during spin coating deposit on Si(111) and Si(100). These domains could play a role on nucleation for crystal growth and stimulate crystallization of reluctant proteins.[12] Furthermore, they may help on the investigation of protein growth and characterization. In particular, this work showed that the protein layer adsorbed on silicon is of the order of one to 6 monolayers depending on depositing protocol. Ordered domains formed during deposit seem to be stable under the X-ray beam. This stability could be due to their small size, reasonable domain order and absence of absorbing atoms in their structure. Grazing incidence X-ray technique is a useful tool especially for angles below total reflection of the substrate and the large illuminating surfaces. Nonetheless, it is shown that the stability of GlnB-Hs protein under 7 keV may not be a limitation factor.

Acknowledgements: The authors are grateful to LNLS Laboratorio Nacional de Luz Sincrotron (LNLS/MCT) for financial support, Dr. Cyro Kretzel, Dr.Guinther Kellermann for beam line support.

[1] J. Gray, *Curr. Opi. in Struct. Biology* **2004**, *14*, 110.
[2] U. Sleytr, E. Gyorvary, *Progr. in Org. Coating* **2003**, *47*, 279.
[3] E. Pechkova, C. Nicolini, *Trends in Bio.* **2004**, *22*, 117.
[4] E. Pechkova, C. Nicolini, *J. of Crystal growth* **2001**, *231*, 599.
[5] R. Giegé, J. Drenth, A. Ducruix, A. McPherson, W. Saenger, *Prog. Cryst. Growth and charact.* **1995**, *30*, 237.
[6] B. K. Jap, M. Zulauf, T. Scheybani, A. Hefti, W. Baumeister, U. Aebi, A. Engel, *Ultramicroscopy* **1992**, *46*, 45.
[7] J. Als-Nielsen, D. Jacquemain, K. Kjaer, F. Leveiller, M. Lahav, L. Leiserowitz, *Physics reports* **1994**, *246*, 251.
[8] M. G. Samant, C. A. Brown, J. G. Gordon II, *Langmuir* **1991**, *7*, 437.
[9] M. Seul, P. Eisenberger, H. M. McCOnnell, *PNAS* **1983**, *80*, 5795.
[10] P. Fenter, P. Eisenberger, J. Li, N. Camillone, S. Bernasek, G. Scoles, T.A. Ramanarayanan, K.S. Liang, *Langmuir* **1991**, *7*, 2013.
[11] T. Salditt, U. Mennicke, *Langmuir* **2002**, *18*, 8172.
[12] S. A. W. Verclas, P. B. Howes, K. Kjaer, A. Wurlitzer, M. Weygand, G. Buldt, N. A. Dencher, M. Losche, *J.M.B.* **1999**, *287*, 837.
[13] C. J. Lawrence, W. Zhou, *J. of Non-Newtonian fluid Mech.* **1991**, *39*, 137.
[14] A. J. Ninfa, M. R. Atkinson, *Trends Microbiol.* **2000**, *8*, 172.
[15] V. L. D. Baldani, J. I. Baldani, F. Olivares, J. Dobereiner, *Symbiosis* **1992**, *13*, 65.
[16] J. I. Baldani, V. L. D. Baldani, L. Seldin, J. Dobereiner, *Int. J. Syst. Bacteriol.* **1986**, *36*, 86.
[17] J. P. Pimentel, F. Olivares, R. M. Pitard, S. Urquiaga, F. Akiba, J. Dobereiner, *Plant Soil* **1991**, *137*, 61.
[18] O. B. Weber, V. L. D. Baldani, K. R. S. Teixeira, G. Kirchhof, J. I. Baldani, J. Doberreiner, *Plant Soil* **1999**, *210*, 103.
[19] E. M. Benelli, E. M. de Souza, S. Funayama, L. U. Rigo, F. O. Pedrosa, *J. Bacteriol.* **1997**, *179*, 4623.
[20] E. M. de Souza, F. O. Pedrosa, M. H. Drummond, L. U. Rigo, M. G. Yates, *J. Bacteriol.* **1999**, *181*, 681.
[21] E. M. Benelli, M. Buck, E. M. de Souza, M. G. Yates, F. O. Pedrosa, *Can. J. Microbiol.* **2001**, *47*, 309.
[22] E. M. Benelli, M. Buck, I. Polikarpov, E. M. de Souza, L. M. Cruz, F. O. Pedrosa, *Eur. J. Biochem.* **2002**, *269*, 3296.
[23] M. Hirose, T. Yasaka, M. Takakura, S. Miyazaki, *Solid State Technology* **1991**, 43.
[24] D. L. Windt, *Computers in physics* **1998**, *12*, 360.
[25] A. F. Lubambo, E. M. Benelli, J. Klein, W. Schreiner, P. C. de Camargo, *Cell Bio. and Biophysics*, **2006**, *44*, 503.
[26] A. Guinier, "*X-Ray Diffraction*", Freeman, San Francisco, **1963**, p. 121.
[27] E. Pechkova, S. Fiodoro, D. Fontani, C. Nicolini, *Acta Crysta. D.* **2005**, *61*, 809.
[28] E. Adachi, K. Nagayama, *Adv. Biophys.* **1997**, *34*, 81.
[29] P. Kralchevsky, N. D. Denkov, *Cur. Opi. In Colloid & Inter. Sci.* **2001**, *6*, 383.
[30] R. Ravelli, S. M. McSweeneney, *Structure* **2000**, *8*, 315.
[31] C. Nave, M. A. Hill, *J. Sync. Rad.* **2005**, *12*, 261.
[32] J. C. Ashley, *IEEE Trans. on Nucl. Scien.* **1980**, *27*, 1454.
[33] M. J. Berger, J. S. Coursey, M. A. Zucker. V 1.2.2., NIST, Gaithersburg, MD, USA **2000**.
[34] P. Hovington, D. Drouin, R. Gauvin, *Scanning* **1997**, *19*, 1.
[35] J. W. Murray, E. F. Garman, R. B. G. Ravelli, *J. of Appl. Cryst.* **2004**, *37*, 513.